

# Investigation on the surface free energy of a single flax fiber through adhesion measurement by atomic force microscopy

Shabbir Ahmed<sup>1</sup>, Xinnan Wang<sup>1</sup>, Kai Li<sup>2</sup> and Chad A Ulven<sup>1</sup>

## Abstract

Surface free energy of a fiber is an important parameter for predicting the interfacial bond strength of fiber-matrix adhesion of composite materials. For mechanical characterization of bio-composite materials, the measurement of the surface energy of individual single microfibers is complicated due to their surface roughness, formation of chemical bonds, wicking characteristics, etc. This paper demonstrates a novel method for determining the dispersive component of surface free energy ( $\gamma_d$ ) of single flax fiber by directly measuring the adhesion force between the probe tip of an atomic force microscope and the fiber surface. Johnson–Kendal–Roberts theory was employed to correlate the adhesion force with the surface energy and tip radius. Finally, the value of  $\gamma_d$  was determined, and its significance with respect to other methods was analyzed.

## Keywords

Flax fiber, surface energy, micro-fibril angle, atomic force microscopy

## Introduction

Flax fibers have been widely used as a reinforcement in bio-composite materials due to their higher strength and modulus, better sound absorption properties, lower specific density, non-toxicity, and lower cost.<sup>1</sup> Flax fibers are derived from the bast or stem of a flax plant, and they are typically a bundle of single fibers called technical fibers. An individual single fiber is an elongated sclerenchyma cell with a diameter of 10–15 µm, forming a complex hierarchical structure and a composite in itself,<sup>2</sup> as shown schematically in Figure 1. Unlike the glass or carbon fiber, the single flax fiber is not a uniform monofilament, but rather has several concentric layers naturally cemented together.

The key to acquire better mechanical performance of composite materials is higher interfacial bonding, which can be achieved by increasing physical adhesion between the fiber and the matrix, and/or by forming a strong chemical bonding, and by better mechanical interlocking. Although the higher roughness of flax fiber provides enhanced mechanical interlocking with the polymeric matrix, the hydrophilicity of the fiber surface may result in weaker interfacial bonding between fiber and matrix.<sup>4–6</sup>

Surface free energy ( $\gamma$ ) of the fiber is an important parameter for quantifying the interfacial bond strength between the fiber and the matrix. One approach for measuring  $\gamma$  of a solid flat surface is to measure the contact angle formed by a liquid droplet on a solid surface. However, the contact angle approach for measuring the surface energy rests on a few assumptions. (1) The solid surface is not chemically affected by the liquid. (2) The contact angles to be measured are true equilibrium angles. (3) The difference between the interfacial surface energy at vacuum ( $\gamma_{sl}^0$ ) and at saturation ( $\gamma_{sl}$ ), known as the spreading pressure ( $\pi_e$ ), is negligible. For most low energy surfaces, on which adsorption is relatively small,  $\pi_e$ , is negligible. (4) Errors due to orientational entropy effects are not important. (5) The solid is free from defects, dislocations, edges, and

<sup>1</sup>Department of Mechanical Engineering, North Dakota State University, USA

<sup>2</sup>Department of Automatic Testing and Control, Harbin Institute of Technology, China

## Corresponding author:

Xinnan Wang, Department of Mechanical Engineering, North Dakota State University, Fargo, ND 58108, USA.  
 Email: xinnan.wang@ndsu.edu

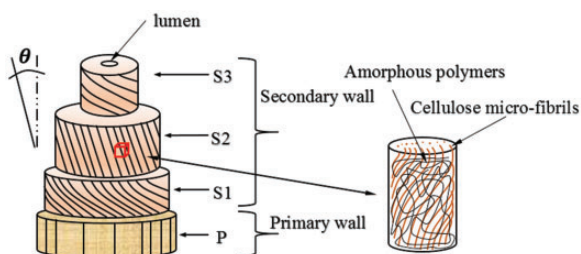


**Figure 1.** Schematic of a single flax fiber with primary and secondary layers. The secondary layer is composed of S1, S2, and S3 layer. A smaller portion of S2 layer is magnified and cellulose micro-fibrils are seen to be dispersed on an amorphous polymeric matrix. Concept adapted from Baley et al.<sup>3</sup>

corners.<sup>7</sup> Schellbach et al.<sup>8</sup> placed two similar diameter fibers in parallel with a spacing of 0.2–1 mm, so that a water droplet placed on them can form a bridge or column. The meniscus of the liquid bridge was then imaged and analyzed for measuring the contact angle which provided better estimates of contact angle than widely used tensiometry<sup>9</sup> and capable of measuring both advancing and receding contact angle.

Another method for measuring the surface energy is the inverse gas chromatography (IGC),<sup>10</sup> which requires the fibers to be grounded in powder form, causing high end values of the surface energy of the materials.<sup>11,12</sup> The zeta potential of a system is correlated to the surface energy of that system and important information could be achieved regarding the nature of the surface through this measurement. Usually, the zeta potential of fibers is measured by streaming potential method where an electrolyte solution is pumped through the fiber bundle. This solution generates a current or potential resulting from the shear of the electrochemical double layer.<sup>13</sup> However, the measurement of zeta potential provides reliable information about surface energy only when the results are corroborated by other physico-chemical methods and the factors influencing the double layers are sufficiently known. Often, the surface conductivity is neglected which causes error in zeta potential measurement, particularly when the fibers are hydrophilic.<sup>14</sup> Moreover, the measurement may be affected by the degree of fiber swelling. Bellmann et al.<sup>15</sup> performed streaming potential experiments by an Electro Kinetic Analyzer (AKA) to study the polarity of fiber surface and swelling behavior of the fiber in water. They found that the higher the cellulose content and crystallinity are, the lower the amount of water adsorbed is. A lower equilibrium value of zeta potential corresponds to a higher adsorption capacity of the fiber. The acid base properties of the fiber surface can also be investigated by the electro-kinetic measurements.<sup>16,17</sup> Recently, atomic force microscopy (AFM) has become a

powerful technique for measuring the surface energy of various polymeric and pharmaceutical materials.<sup>18,19</sup> This method has also been proved successful for the characterization of cellulosic fibers.<sup>20,21</sup> Pietak et al. investigated the surface properties of hemp fibers through AFM. They treated the hemp fibers in four different ways: steam, alkaline, combination of steam-alkaline, and enzymatic treatments and determined the variation of surface free energies among these four types of fibers. They also measured the contact angle formed by different liquids with these fibers, and predicted a relationship among the water contact angle, adhesion force, and surface free energy. However, no attempt is taken in the literature, according to the knowledge of the authors, to measure the surface energy of a single flax fiber by AFM. In this study, the adhesion force between the AFM tip and the single flax fiber was measured by AFM and correlated to the contact mechanics models for determining the dispersive component of surface free energy of single flax fibers.

## Materials and methods

Flax fiber used in this study were Prairie Grande Flax, a medium early maturing oilseed flax (*Linum usitatissimum* L.), grown in Melita, Manitoba, Canada. At harvest, the average height of the plants were 60 cm, and observed to be dry or fully mature.

Enzyme retting was performed for extracting the fiber from the cuticularized epidermis and the woody core cells. Bioprep 3000L was used as the enzyme which is an alkaline pectate lyase. Flax stems were fully immersed in a 5% Bioprep 3000L plus Sodium Tetraborate Decahydrate (buffer) for 30 min at  $21 \pm 2^\circ\text{C}$ . Next, the stems were taken out and allowed to dry in oven at  $55^\circ\text{C}$  for 2 h.

After that the stems were again immersed in ethylenediamine tetraacetic acid (EDTA) plus buffer for 30 min at  $21 \pm 2^\circ\text{C}$ . Then, the stems were taken out and dried in the oven for 22 h at  $55^\circ\text{C}$ . The stems were then rinsed with water for 5 min and dried overnight in the fume hood.

The single fibers were carefully hand separated from the bundle and laid down on a glass slide coated with a thin layer of partially cured epoxy. The coating was deposited on the glass slide on such a time that the viscosity of the resin system is high enough not to flow. Only the lower part of the single fiber was in contact with the resin and the upper part was free from any contaminants. The resin was then left to cure for 24 h and the lower part of the fiber was firmly fixed with glass slide through the epoxy resin. As a result, during the measurement of the force distance curve, the fibers were rigidly supported by the glass slide.

Figure 2 schematically shows the adhesion measurement by AFM. In an ideal case, a perfectly smooth surface would be preferred for measuring the surface energy. However, as a natural fiber, the flax fiber offers limited opportunity for the manual surface finish, therefore, measuring the surface energy of a single flax fiber in its natural state was desired. A smooth region of the fiber was selected for each indentation.

Adhesion force measurements were performed using an AFM (Veeco, D3100) tapping mode at 23°C and 40% relative humidity (RH). The AFM probe used was from MicroMasch with the model NSC15 and made from n-type silicon. The cantilever had a length and width of 125 µm and 30 µm, respectively, with a resonance frequency of 320 kHz and a quality factor of 657. To convert the AFM cantilever deflection into its corresponding force component, the spring constant of the cantilever needed to be measured. Several methods are available for calculating the spring constant of the AFM probe, such as the thermal fluctuation measurement method, the kinetostatic method, the heterodyne interferometry method, and the extended added micro-drop method.<sup>22–24</sup> The Sader method<sup>25</sup> was used

here for determining the spring constant and calculated to be 37.5 N/m. The tip of the cantilever was characterized by Field Emission Scanning Electron Microscopy (FESEM) (JEOL JSM-7600F). The predetermined nanoindentation load on the fiber was 180 nN. The indentation was performed at 10 different locations of the flax fiber. The neighboring indentation distances were at least 500 nm apart to avoid the effect of adjacent deformations on the fiber. The corresponding reaction force vs. z-piezo displacement curve was recorded. The z-piezo displacement curve after the tip-sample contact was a combination of the sample deflection and the cantilever deflection.

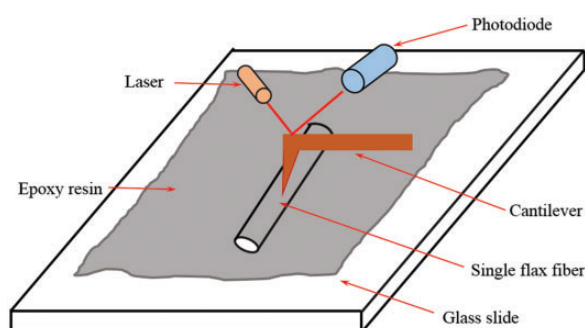
## Results and discussion

Figure 3(a) reveals an FESEM image of the surface of a single flax fiber. The surface is nearly smooth except for a few localized inclusions. In Figure 3(b), AFM was used for numerical quantification of the surface roughness, and the root mean square value of the surface roughness of the single fiber was determined to be 25 nm within a 1.5 µm × 1.5 µm area.

Figure 3(b) reveals some of the intricate details such as the meso-fibrils of a single flax fiber. Although the mesofibrils in the S2 layer is covered by the primary layer and the S1 layer, it is possible to probe those meso-fibrils by AFM. The dimensions of these meso-fibrils of flax fibers vary from 0.5 to 1.5 µm. There exist tiny grooves in between the regions from one meso-fibril to another. These grooves may contribute to a higher surface roughness of a single flax fiber.

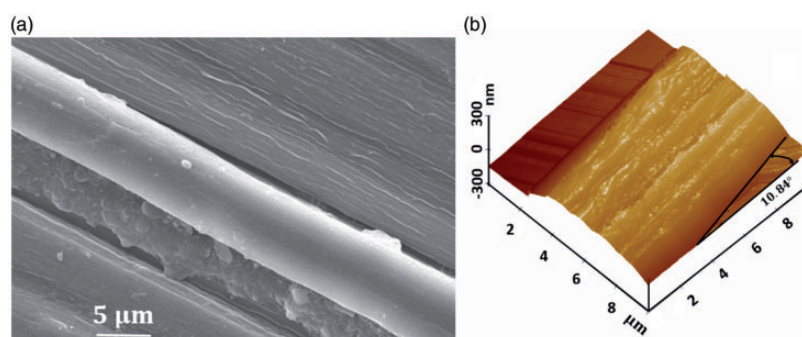
The meso-fibril angle of a single flax fiber determined by AFM was found to be approximately 11°. A lower meso-fibril angle is responsible for lower strain but higher strength and modulus.<sup>2</sup>

Figure 4(a) shows an FESEM image of the side view of the silicon AFM tip used in this experiment. A magnified view of the tip (Figure 4(b)) shows that the tip



**Figure 2.** Schematic representation of the adhesion measurement process by AFM.

AFM: atomic force microscopy.



**Figure 3.** (a) FESEM image of a localized surface topography of a single flax fiber. (b) AFM 3D image of individual visible meso-fibrils. FESEM: field emission scanning electron microscopy; AFM: atomic force microscopy.

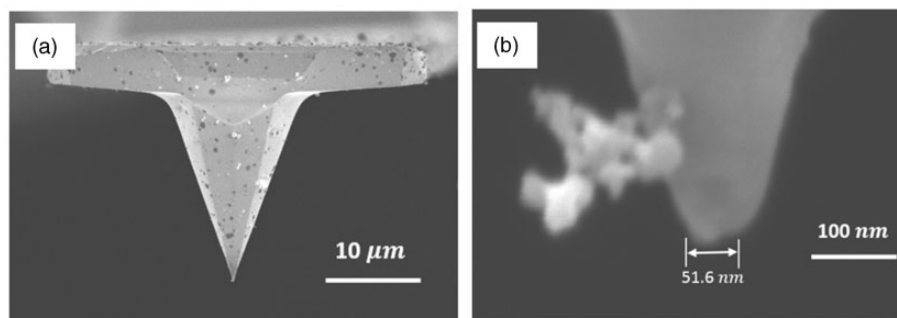


**Figure 4.** (a) FESEM image of the AFM tip, and (b) magnified view of the tip diameter.  
FESEM: field emission scanning electron microscopy; AFM: atomic force microscopy.

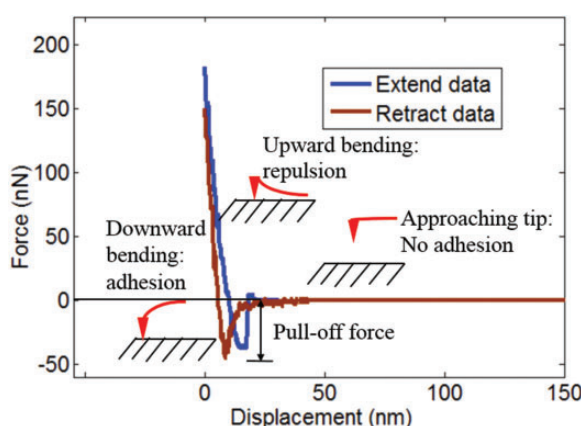


**Figure 5.** Force vs. displacement curve of the single flax fiber showing the pull-off force arising from the adhesion between the fiber surface and the probe tip.

radius is 25 nm, which correlates the adhesion force and the surface energy.

Figure 5 depicts the tip-surface interaction during the measurement of the adhesion force. When the two surfaces are close enough on the order of several nanometers, the short range van der Waals forces, both electrostatic and attractive in nature, become activated between the surface molecules, and they attract each other. This attraction phenomenon is generally referred to as the adhesion between the surfaces. When two surfaces are in contact due to this adhesion force, a certain amount of force is required to separate them. This separation force is known as the pull-off force, an indirect measure of the adhesion force present between the surfaces. When the tip was far from the surface, there was no interaction between the fiber and the tip. As the tip further approached to the fiber surface, due to the short-range van der Waals force, the tip had a sudden snap-in towards the surface. As the cantilever continued to be pushed down, the adhesion force decreased to zero, and the compressive force became activated. The blue curve represents the extend data, which were

recorded when the AFM cantilever tip was approaching and indenting the sample, and the magenta curve represents the retract data, which were recorded when the AFM cantilever tip was retracting from the sample surface after the interaction. The region of the extension curve below the zero line represents the magnitude of the pull-off force or adhesion force, which was found to be  $47.8 \pm 12.5$  nN. The measurement procedure is described in the Materials and Method section in detail.

Again from Figure 5, it can be observed that the value of the pull-off force in retract curve is slightly higher than that of the extend curve. Ideally, the value of the pull-off force from these two curves should be equal for linear elastic materials. However, most polymers are viscoelastic in nature and their load-deformation curve is sensitive to strain rate. Moreover, they show adhesion hysteresis, that is, more work is required to separate the contacting surfaces than the adhesion force required to bring them in contact. This may explain a bigger pull off force required for the retract data. A detailed analysis of the viscoelastic nature of polymeric materials was presented in Wahl et al.<sup>26</sup> They showed that the discrepancy between the experimental stiffness and theoretical stiffness predicted by the Johnson-Kendall-Roberts (JKR) model can be accounted for by employing a model that incorporates this viscoelastic effect at the periphery of the contact zone.

Contact mechanics models were employed for calculating the surface energy from the pull-off force. There are several models correlating the adhesion force to that of the surface free energy of the contacting materials. Among them JKR model<sup>27</sup> and Derjaguin-Muller-Toporov (DMT) model<sup>28</sup> are the most prominent. JKR model was derived by considering two elastic spheres in contact under zero external force. It was assumed that attractive force due to adhesion was present between the two spheres, and this establishes a finite contact radius. By performing numerical simulations of Lennard-Jones potential, Muller et al.<sup>29,30</sup> showed that JKR and DMT are two limiting models of the adhesion force. JKR model is more appropriate

when the radius of the AFM tip is larger and the material being probed is more compliant. This model takes into account only the strong adhesion force under the tip in contact with the object. On the other hand, DMT model is appropriate when the probe tip radius is small and the material being probed is stiff. This model also takes into account the long range weak adhesion force present between the periphery of the probe near the surface in addition to the strong adhesion force present under the tip in contact with the surface of the object.

Usually, two non-dimensional physical parameters, Tabor's parameter  $\mu$ ,<sup>31</sup> and Maugis parameter  $\lambda$ ,<sup>32,33</sup> are used to quantify the transition between JKR and DMT models. They are related by the equation  $\lambda = 1.1570\mu$ , where

$$\mu = \left( \frac{16Rw^2}{9K^2z_0^3} \right)^{1/3} \quad (1)$$

$$\lambda = 2\sigma_0 \left( \frac{R}{\pi K^2 w} \right)^{1/3} \quad (2)$$

where  $z_0$  is the equilibrium separation of surfaces,  $R$  is the tip radius,  $w$  is the interfacial energy per unit area or work of adhesion,  $K$  is the combined elastic modulus of the tip and the sample, given by  $K = \frac{4}{3}((1 - \nu_1^2)/E_1 + (1 - \nu_2^2)/E_2)^{-1}$ , where  $E_1$  and  $E_2$  are the tip and the sample Young's modulus, respectively, and  $\nu_1$  and  $\nu_2$  are the Poisson ratio of the tip and the sample, respectively.  $\sigma_0$  is the constant adhesive stress acting over a range  $\delta_0$  in Dugdale square well potential model. If  $\lambda > 5$ , then JKR model is more appropriate and if  $\lambda < 0.1$ , DMT model applies.

In the present experiment, the elastic modulus of the probe tip  $E_1 = 165.1$  GPa,  $E_2 = 50$  GPa,  $\nu_1 = 0.223$ ,  $\nu_2 = 0.1$ ,<sup>34</sup>  $z_0 = 0.6$  nm, and  $w = 178$  nJ/nm<sup>2</sup>.<sup>35</sup> Thus  $\mu = 16.06$ , and  $\lambda = 18.577 > 5$ , as  $\lambda = 1.1570\mu$ . As a result, JKR model is more appropriate here for calculation of surface energy.

For the calculation of surface free energy, the pull-off force from the extend data and the equations from JKR model were used.

$$F_{(pull-off)} = -\frac{3}{2}\pi RS \quad (3)$$

$$S = 2\sqrt{\gamma_1^d \gamma_2^d} \quad (4)$$

where  $\gamma_1^d$  and  $\gamma_2^d$  are the dispersive component of the surface energy of the tip and the sample, respectively. The surface energy of the silicon was used as 1250 mJ/m<sup>2</sup>.<sup>36</sup> Thus, the dispersive component of the

**Table 1.** Comparison of the dispersive component of surface energy values with different methods.

Method	$\gamma_2^d$ (mJ/m <sup>2</sup> )	Materials	Sample preparation
IGC <sup>37</sup>	43.1	Flax fiber	Sample needs grounded in powder form. High energy sites are probed.
IGC <sup>38</sup>	41	Untreated jute	
IGC <sup>38</sup>	37	Silane treated jute	
Capillary rise <sup>38</sup>	23	Jute fibers	Grounded sample is tightly packed into a holder. Gravity may influence the results
Capillary rise <sup>39</sup>	29.2	Flax fiber	
<sup>40</sup>	27.5–50	Flax fiber	
Capillary rise <sup>41</sup>	24	Flax fiber	

IGC: inverse gas chromatography.

surface energy of a single flax fiber was found to be  $32.9 \pm 2.1$  mJ/m<sup>2</sup>.

The obtained value of the dispersive component of the surface free energy of a single flax fiber agrees well with other published literature values that are listed in Table 1. It should be noted that the underlying principles used to determine the surface free energy among different methods can be different. In general, the measurement of surface energy of single flax fiber is subjected to the method of separation of fibers, surface treatment applied on the fibers, degree of retting, and the method of measurement used.

During the measurement of adhesion force by AFM, with the presence of humidity, the adhesion force between the probe tip and the sample surface is mainly governed by the short range van der Waals force and the capillary force.<sup>42</sup> The situation may be more complicated due to the presence of electrostatic force and the formation of chemical bonding.<sup>43</sup> Due to the presence of high humidity, the sample surface is generally covered by a thin water film. This thin film may form a capillary bridge between the probe tip and the sample surface; therefore, the capillary force would be superimposed with other interactions such as van der Waals force.<sup>44,45</sup> However, the effect of this capillary force is subjected to the wettability of water to the sample surface and the probe tip. A hydrophobic sample surface would result in a very small capillary force. Binggeli et al.<sup>46</sup> studied the condensation of water around an AFM probe in contact with a flat surface. They found that a relative humidity of less than 75% has little effect on the capillary force. However, as the surrounding environment approaches to the point of saturation, significant capillary condensation occurs which affects nano-scale properties. A hydrophilic surface may expedite this process. Again, when the radius of curvature of the probe tip

is large enough, the effect of capillary condensation is negligible.<sup>47</sup>

As the relative humidity of the laboratory was maintained at around 40% RH and the radius of the probe tip was large enough, it is expected that the effect of capillary condensation is negligible. To minimize the effect of electrostatic force during adhesion force measurement, the experimental setup was periodically discharged and ground connected to prevent the buildup of excess charge. As a result, the effect of electrostatic force was also negligible. The single flax fibers were dry enough to prevent the formation of chemical bonding such as hydrogen or hydrophilic bonding between the tip and the fiber surface. Hence, the adhesion force measured by AFM is expected to be arising from mainly due to the van der Waals interactions between the probe tip and the fiber surface.

## Conclusion

In this work, the dispersive component of surface free energy of a single flax fiber was determined by AFM through the direct measurement of fiber-tip adhesion force. The value of  $\gamma_2^d$  was evaluated to be  $32.9 \pm 2.1 \text{ mJ/m}^2$ . Compared with other measurement methodologies, AFM is proven to be a powerful tool in measuring the surface free energy of flax fibers. No additional surface preparation is required and flax fibers are in its natural state, which is essential for understanding its surface characteristics for manufacturing bio-composite materials. The measurement of adhesion force may also predict the surface wettability of single flax fibers. Thus, the method shown in this paper may serve as a useful tool for investigating the fiber-matrix adhesion properties of natural fiber reinforced composite materials.

## Author's contributions

S Ahmed prepared the sample, carried out the experiment, analyzed data, and drafted the manuscript. X Wang and C Ulven supervised and guided the overall project and involved in drafting the manuscript. K Li performed the MATLAB coding and involved in sample preparation.

## Declaration of Conflicting Interests

The author(s) declared no potential conflicts of interest with respect to the research, authorship, and/or publication of this article.

## Funding

The author(s) disclosed receipt of the following financial support for the research, authorship, and/or publication of this article: Funding support is provided by Composite Innovation Center (CIC), Winnipeg, Canada, and North Dakota Department of Commerce.

## References

1. Fuqua MA, Huo S and Ulven CA. Natural fiber reinforced composites. *Polym Rev* 2012; 52: 259–320.
2. Burgert I and Dunlop JW. Micromechanics of cell walls. In: *Mechanical integration of plant cells and plants*. Springer-Verlag Berlin Heidelberg, 2011, pp.27–52.
3. Baley C, et al. Influence of drying on the mechanical behaviour of flax fibres and their unidirectional composites. *Compos Part A Appl Sci Manuf* 2012; 43: 1226–1233.
4. Zafeiropoulos NE, et al. Engineering and characterisation of the interface in flax fibre/polypropylene composite materials. Part I. Development and investigation of surface treatments. *Compos Part A Appl Sci Manuf* 2002; 33: 1083–1093.
5. Zafeiropoulos NE, Baillie CA and Hodgkinson JM. Engineering and characterisation of the interface in flax fibre/polypropylene composite materials. Part II. The effect of surface treatments on the interface. *Compos Part A Appl Sci Manuf* 2002; 33: 1185–1190.
6. Bismarck A, et al. Surface characterization of natural fibers; surface properties and the water up-take behavior of modified sisal and coir fibers. *Green Chem* 2001; 3: 100–107.
7. Girifalco L and Good R. A theory for the estimation of surface and interfacial energies. I. Derivation and application to interfacial tension. *J Phys Chem* 1957; 61: 904–909.
8. Schellbach SL, Monteiro SN and Drelich JW. A novel method for contact angle measurements on natural fibers. *Mater Lett* 2016; 164: 599–604.
9. Sauer BB and Carney TE. Dynamic contact angle measurements on glass fibers: influence of fiber diameter on hysteresis and contact line pinning. *Langmuir* 1990; 6: 1002–1007.
10. Yampolskii Y and Belov N. Investigation of polymers by inverse gas chromatography. *Macromolecules* 2015; 48: 6751–6767.
11. Newell HE, et al. The use of inverse phase gas chromatography to measure the surface energy of crystalline, amorphous, and recently milled lactose. *Pharm Res* 2001; 18: 662–666.
12. Ahfat NM, et al. An exploration of inter-relationships between contact angle, inverse phase gas chromatography and triboelectric charging data. *Eur J Pharm Sci* 2000; 9: 271–276.
13. Stokes RJ and Evans DF. *Fundamentals of interfacial engineering*. New York, NY: John Wiley & Sons, 1997.
14. Jacobasch H-J, Bauböck G and Schurz J. Problems and results of zeta-potential measurements on fibers. *Colloid Polym Sci* 1985; 263: 3–24.
15. Bellmann C, et al. Electrokinetic properties of natural fibres. *Colloids Surfaces A Physicochem Eng Asp* 2005; 267: 19–23.
16. Pothan LA, et al. Determination of polarity parameters of chemically modified cellulose fibers by means of the solvatochromic technique. *J Polym Sci Part B Polym Phys* 2000; 38: 2546–2553.
17. Gutmann V. *Donor-acceptor approach to molecular interactions*. New York, NY: Plenum Press, 1978.

18. Louey MD, Mulvaney P and Stewart PJ. Characterisation of adhesional properties of lactose carriers using atomic force microscopy. *J Pharm Biomed Anal* 2001; 25: 559–567.
19. Roberts CJ. What can we learn from atomic force microscopy adhesion measurements with single drug particles?. *Eur J Pharm Sci* 2005; 24: 153–157.
20. Magonov SN and Reneker DH. Characterization of polymer surfaces with atomic force microscopy. *Annu Rev Mater Sci* 1997; 27: 175–222.
21. Bastidas JC, et al. Chemical force microscopy of cellulosic fibers. *Carbohydr Polym* 2005; 62: 369–378.
22. Tseytlin YM. Atomic force microscope cantilever spring constant evaluation for higher mode oscillations: a kinetostatic method. *Rev Sci Instrum* 2008; 79: 025102.
23. Torii A, et al. A method for determining the spring constant of cantilevers for atomic force microscopy. *Meas Sci Technol* 1996; 7: 179–184.
24. Golovko DS, et al. Nondestructive and noncontact method for determining the spring constant of rectangular cantilevers. *Rev Sci Instrum* 2007; 78: 043705.
25. Sader JE, et al. Method for the calibration of atomic force microscope cantilevers. *Rev Sci Instrum* 1995; 66: 3789–3798.
26. Wahl K, et al. Oscillating adhesive contacts between micron-scale tips and compliant polymers. *J Colloid Interface Sci* 2006; 296: 178–188.
27. Johnson K, Kendall K and Roberts A. Surface energy and the contact of elastic solids. In: *Proceedings of the Royal Society of London A: Mathematical, Physical and Engineering Sciences*. London, England: The Royal Society, 1971.
28. Derjaguin BV, Muller VM and Toporov YP. Effect of contact deformations on the adhesion of particles. *J Colloid Interface Sci* 1975; 53: 314–326.
29. Muller V, Yushchenko V and Derjaguin B. On the influence of molecular forces on the deformation of an elastic sphere and its sticking to a rigid plane. *J Colloid Interface Sci* 1980; 77: 91–101.
30. Muller VM, Yushchenko VS and Derjaguin BV. General theoretical consideration of the influence of surface forces on contact deformations and the reciprocal adhesion of elastic spherical particles. *J Colloid Interface Sci* 1983; 92: 92–101.
31. Tabor D and Winterton R. The direct measurement of normal and retarded van der Waals forces. In: *Proceedings of the Royal Society of London A: Mathematical, Physical and Engineering Sciences*. London, England: The Royal Society, 1969.
32. Maugis D. Adhesion of spheres: the JKR-DMT transition using a Dugdale model. *J Colloid Interface Sci* 1992; 150: 243–269.
33. Carpick RW, Ogletree DF and Salmeron M. A general equation for fitting contact area and friction vs load measurements. *J Colloid Interface Sci* 1999; 211: 395–400.
34. Baley C. Analysis of the flax fibres tensile behaviour and analysis of the tensile stiffness increase. *Compos Part A Appl Sci Manuf* 2002; 33: 939–948.
35. Hurley D and Turner JA. Measurement of Poisson's ratio with contact-resonance atomic force microscopy. *J Appl Phys* 2007; 102: 033509.
36. Jaccodine R. Surface energy of germanium and silicon. *J Electrochem Soc* 1963; 110: 524–527.
37. Heng JY, et al. Methods to determine surface energies of natural fibres: a review. *Compos Interfaces* 2007; 14: 581–604.
38. Gassan J, Gutowski VS and Bledzki AK. About the surface characteristics of natural fibres. *Macromol Mater Eng* 2000; 283: 132–139.
39. Aranberri-Askargorta I, Lampke T and Bismarck A. Wetting behavior of flax fibers as reinforcement for polypropylene. *J Colloid Interface Sci* 2003; 263: 580–589.
40. Van Hazendonk J, et al. A simple experimental method for the measurement of the surface tension of cellulosic fibres and its relation with chemical composition. *Colloids Surfaces A Physicochem Eng Asp* 1993; 81: 251–261.
41. Cantero G, et al. Effects of fibre treatment on wettability and mechanical behaviour of flax/polypropylene composites. *Compos Sci Technol* 2003; 63: 1247–1254.
42. Van Honschoten J, Tas N and Elwenspoek M. The profile of a capillary liquid bridge between solid surfaces. *Am J Phys* 2010; 78: 277–286.
43. Sedin DL and Rowlen KL. Adhesion forces measured by atomic force microscopy in humid air. *Anal Chem* 2000; 72: 2183–2189.
44. Eastman T and Zhu D-M. Adhesion forces between surface-modified AFM tips and a mica surface. *Langmuir* 1996; 12: 2859–2862.
45. Moon S-H and Foster MD. Influence of humidity on surface behavior of pressure sensitive adhesives studied using scanning probe microscopy. *Langmuir* 2002; 18: 8108–8115.
46. Binggeli M and Mate C. Influence of capillary condensation of water on nanotribology studied by force microscopy. *Appl Phys Lett* 1994; 65: 415–417.
47. Sugawara Y, et al. Effects of humidity and tip radius on the adhesive force measured with atomic force microscopy. *Wear* 1993; 168: 13–16.